A HYBRID UTD-EIGENFUNCTION METHOD FOR SCATTERING BY A VERTEX[1]

John N. Sahalos
Department of Physics
University of Thessaloniki
Thessaloniki 54006, Greece

and

Gary A. Thiele
F.M. Tait Professor of Electrical Engineering
University of Dayton
Dayton, OH 45469-0227

ABSTRACT

Present solutions for the electromagnetic scattering by a vertex are either approximate or difficult to use for computations. For example, GTD (UTD) solutions for vertex scattering are not yet fully developed. The exact eigenfunction solution is both difficult to use and computationally inefficient due to the large number of eigenfunctions that must be retained.

In this work, we obtain the scattering by a vertex (e.g., a quarter plane) by employing the exact eigenfunction solution only in a very small region close to the tip of the vertex. Thus, only a small number of eigenfunctions (e.g., two or three) are required to obtain the current in the tip region. Outside of this region, the UTD is employed to obtain the current. The changeover point is determined by finding the point where the eigenfunction current has decayed to that predicted by UTD wedge and vertex diffraction theory.

Results will be shown for the scattered field from the plane angular sector. In addition, the field scattered by a rectangular plate using this method will be compared with that predicted by the UTD with vertex diffraction, and the results will be seen to be in very close agreement.

---

[1]The work reported in this paper was supported in part by Contract F19628-78-C-0198 between Electronic Systems Division, Hanscom Air Force Base, Massachusetts, and The Ohio State University Research Foundation and by NATO Research Grant NG 1455.

I. INTRODUCTION AND FORMULATION

The purpose of this paper is to combine the eigenfunction solution with UTD wedge diffraction theory to obtain the current on a plane angular sector using only two or three eigenfunctions. The use of only a few eigenfunctions is possible because the eigenfunction solution is used to find the current only in the region very close (i.e., $r \approx 0.1\lambda$) to the vertex. The UTD is then used to determine the current everywhere else. Results will be shown for the far field when the angular sector is illuminated by a short dipole. The angular sector work here will be used with superposition and the UTD to find the current on four-sided thin plates.

The exact eigenfunction solution to electromagnetic scattering by a vertex was introduced by Satterwhite and Kouyoumjian [1] and by Satterwhite [2]. The eigenfunctions and eigenvalues in this paper were found from application of methods described in [1], although an alternative approach may be found in [3].

The eigenfunction solution can be found by separation of variables in sphero-conal coordinates [1-5]. A plane angular sector is a coordinate surface of the sphero-conal system and it's angle is determined by an ellipticity parameter k^2. The sphero-conal system is described by three coordinate surfaces which are a sphere, an elliptic cone and an elliptic half cone. The r, θ, ϕ coordinates are related to the cartesian x,y,z by the following equations.

$$\left.\begin{aligned} x &= r\cos\theta\sqrt{1-k'^2\cos^2\phi} \\ y &= r\sin\theta\sin\phi \\ z &= r\cos\phi\sqrt{1-k^2\cos^2\theta} \end{aligned}\right\} \tag{1}$$

where $k'^2 = 1 - k^2$, $0 \le k^2 \le 1$, $0 \le \theta \le \pi$ *and* $0 \le \phi \le 2\pi$. The current on the angular sector due to the current density $\bar{J}$ is determined by the dyadic Green's function $\Gamma(\bar{R}, \bar{R}')$ which is given in [1] and [2]. It is:

$$\bar{J}(\bar{R}) = \hat{n} \times [\bar{H}(r, \theta = \pi, 0 < \phi < \pi) - \bar{H}(r, \theta = \pi, \pi + \phi)] \tag{2}$$

where the magnetic field $\bar{H}(\bar{R})$ is

$$\bar{H}(\bar{R}) = -\nabla \times \int_v \Gamma(\bar{R}, \bar{R}') \cdot \bar{J}(\bar{R}') \cdot dv \tag{3}$$

An investigation of the eigenvalues and eigenfunctions of the problem shows that the current on the plane angular sector is a function of the even Dirichlet (01) and the odd Neumman (02) functions. For the even Dirichlet the current distribution from one eigenfunction is:

$$\bar{J}_{el}\, BZ_{\nu_{el}}(\kappa r)\, \frac{\phi_{el}(\varphi)}{\sin\phi}\, \hat{r} \tag{4}$$

and for the odd Neumman it is:

$$\bar{J}_{02} = A\, \frac{[rZ_{\nu_{02}}(\kappa r)]'}{\kappa r} \left[-\phi_{02}(\varphi)\, \hat{\varphi} + \frac{1}{\nu_{02}}\, \frac{\sqrt{1-k^2\cos^2\phi}}{k'\sin\varphi}\, \phi_{02}(\phi)\, \hat{r} \right] \tag{5}$$

The $Z_\nu(\kappa r)$ function is the spherical Bessel function which becomes $h_\nu^{(2)}(\kappa r)$ for $r \geq r_0$ *and* $j_\nu(\kappa r)$ *for* $r \leq r_0$ (r_0 is the distance of the source from the origin). A and B are complex coefficients which depend on the location and the direction of the current source. κ is the wavenumber of the isotropic medium surrounding the plane angular sector.

For $r << \lambda$ the expression of the current will depend on the $j_\nu(\kappa r)$ functions with small values of ν. That is because for $\kappa r << 1$ we have:

$$j_\nu(\kappa r) \propto r^\nu \tag{6}$$

and

$$\frac{[rj_\nu(\kappa r)]'}{\kappa r} \propto r^{\nu-1} \tag{7}$$

Thus, the dominant current near the tip could be given by using the first few eigenfunctions. For example, if we have a unit dipole source located as in Figure 1a, it was found that one must include the first nonzero Neumman eigenfunction in order to obtain a contribution to the $\hat{\phi}$ directed current. It is also found that the $\hat{r}$ directed current changes significantly for this eigenfunction, and actually is the dominant term as the dipole is moved further out from the tip.

In Figures 1b and c we can see the magnitude of the current distribution for two different distances from the tip versus the azimuthal angle along the angular sector found by using the first three or four eigenfunctions.

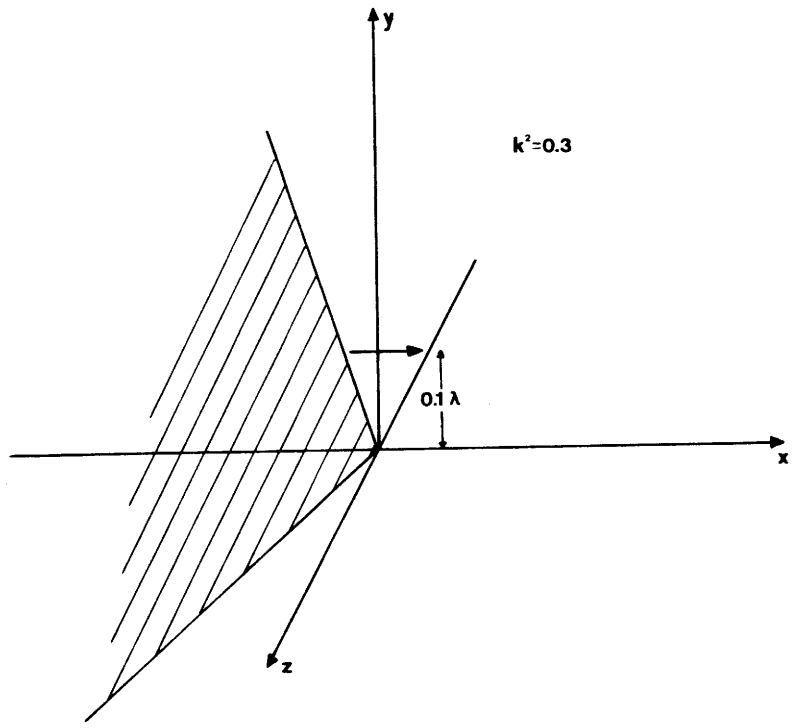

Figure 1a Unit dipole source located near a plane sector in the xz plane.

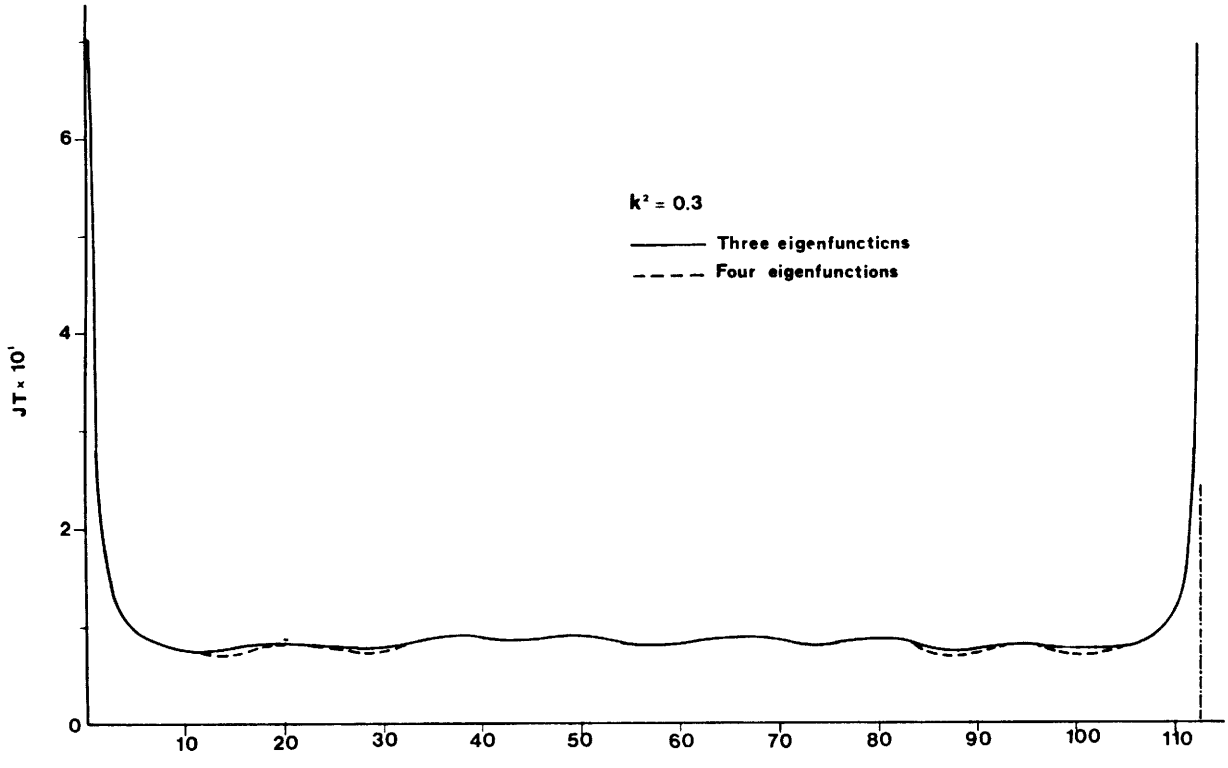

Figure 1b Total current distribution vs. azimuthal angle along the plane angular sector for a distance r = 0.009λ from the tip due to a unit dipole located as in Figure 1a.

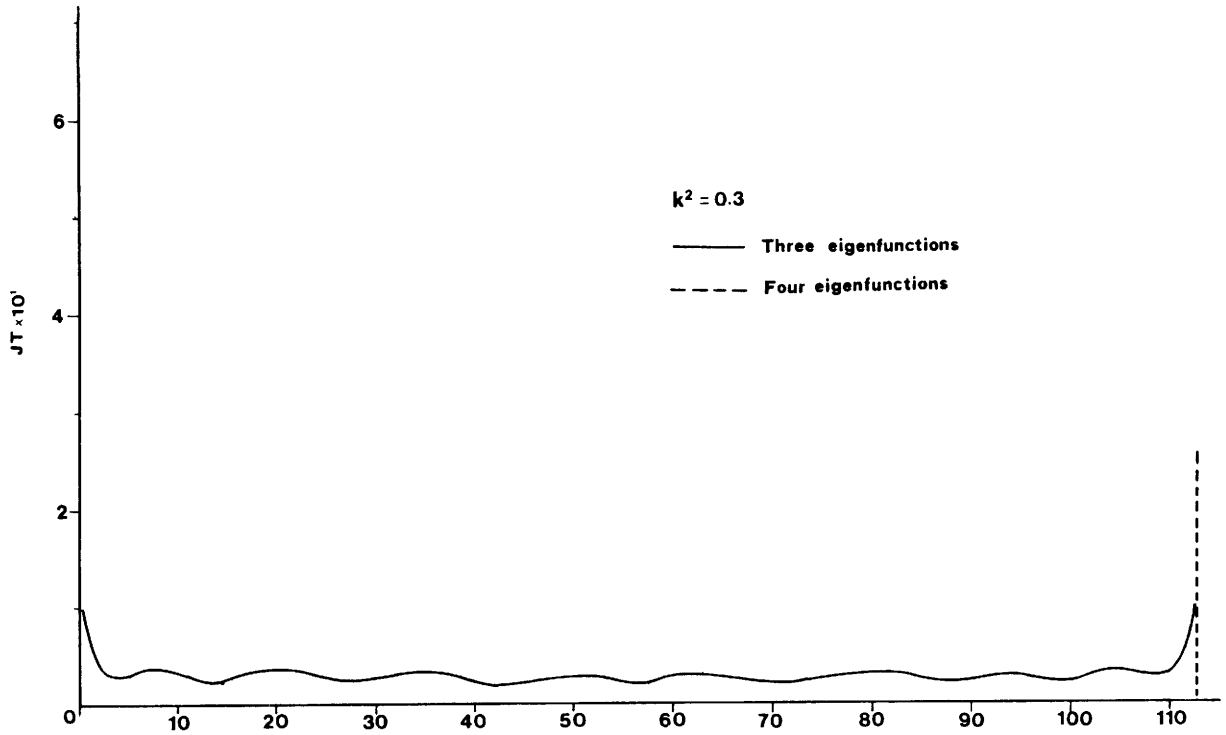

Figure 1c Total current distribution vs. azimuthal angle along the plane angular sector for a distance r = 0.01λ from the tip due to a unit dipole located as in Figure 1a (the two curves are identical).

As we can see, the fourth eigenfunction contributes less than 1% and so we can use only the first three with good accuracy. k^2 is the ellipticity parameter of the sector.

Far from the tip ($\kappa r >> 1$) we could express the tip diffracted current with the help of Equations (4) and (5) in the form:

$$\bar{J}_{TD} = \frac{e^{-j\kappa r}}{\kappa r}\left[\frac{\varphi_1(\phi)}{\sin\phi}\,\hat{r} + \varphi_2(\phi)\,\hat{\phi}\right] \tag{8}$$

where the functions $\varphi(\phi)$ are:

$$\varphi_1(\phi) = A_0 + A_1\cos\phi + A_2\cos 2\phi + \ldots \tag{9}$$

$$\varphi_2(\phi) = B_1\sin\phi + B_2\sin 2\phi\; B_3\sin 3\phi + \ldots \tag{10}$$

The unknown coefficients A_i and B_i can be found by using the EFIE to generate two systems of linear equations using point-matching. The EFIE is

$$\hat{n} \times \bar{e}^{inc} = \frac{1}{4\pi j\omega\epsilon} \hat{n} \times \int_s (-\omega^2\mu\epsilon\bar{J}_s\, G + \nabla_s \bar{J}_s \cdot \nabla' G)\, ds \tag{11}$$

where G is the free space Green's function and $\bar{J}_s$ in this problem is given by:

$$\left.\begin{aligned} \bar{J}_s &= \bar{J}_{total} && 0 \le \kappa r \le 1 \text{ (see eqs. (4) and (5))} \\ \bar{J}_s &= \bar{J}^{GO} + \bar{J}_{edges} + \bar{J}_{TD} && \kappa r \ge 1 \end{aligned}\right\} \tag{12}$$

or in words, for $\kappa r \ge 1$ the current is the sum of the geometrical optics current, the diffracted current from the edges and the tip diffracted current, respectively.

II. ANGULAR SECTOR RESULTS

By using the EFIE with just three sample points, we found the six unknowns in the tip diffracted current expressions in Equations (9) and (10). The integration of EFIE was terminated 20λ from the sample point since the integrated functions go quickly to zero with distance. The sample point locations were investigated regarding the sensitivity of the coefficients in the tip diffracted current expressions. It was found that for distances more than 1λ from the tip the results taken for the coefficients A_i, B_i are approximately the same. In Figures 2, 3, and 4 we can see the total field for an infinitesimal dipole located near the angular sector and normal to it. The field is given for several ellipticity parameters (i.e., $k^2 = 0.5, 0.6, 0.7, 0.8, 0.9$). The distance from the tip is $\kappa r_0 = 2.0$ *with* $\theta_0 = \pi$ *and* $\phi_0 = \frac{\pi}{2}$. Our result for $k^2 = 0.5$ is in good agreement with those given by Satterwhite [2].

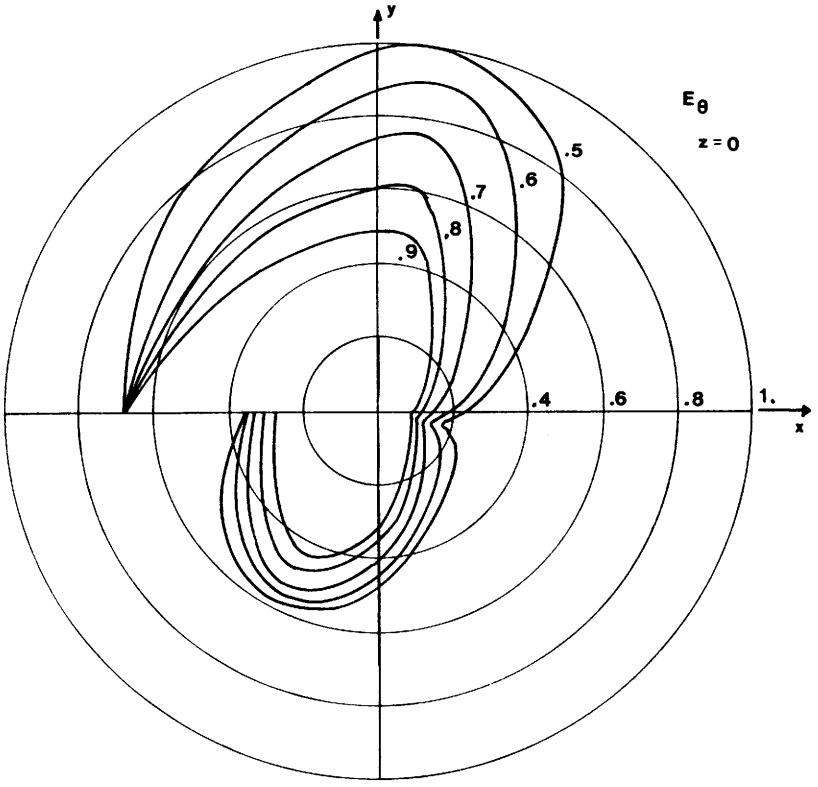

Figure 2 E_θ field on z = 0 plane for five different angular sectors, k^2 = 0.5 to 0.9.

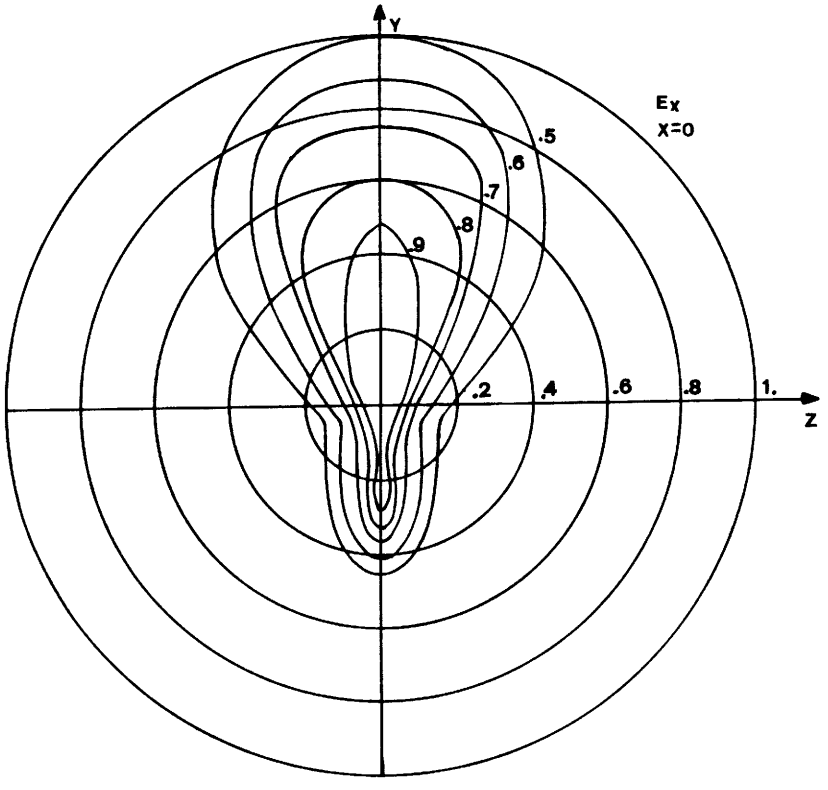

Figure 3 E_x field on x = 0 plane for five different angular sectors, k^2 = 0.5 to 0.9.

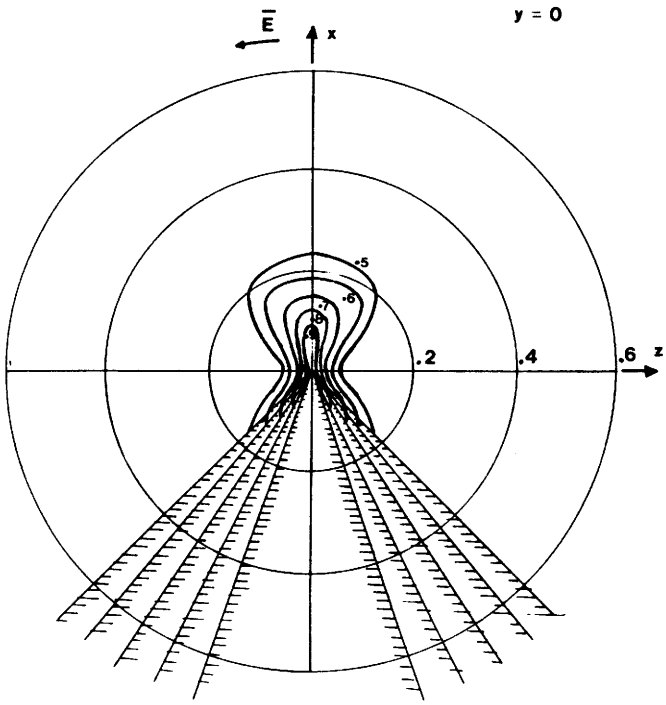

Figure 4 Total electric field y = 0 plane for five different angular sectors, $k^2 = 0.5$ to 0.9.

III. FINITE THIN PLATES

A finite thin plate has both edges and vertices. We can use the angular sector solution and the UTD to obtain the currents. The current distribution expression is given by superposition. For example a finite thin plate with N vertices has a current distribution given by:

$$\left.\begin{aligned} \bar{J}^i &= \bar{J}_{total} + \sum_{j=1}^{N} \bar{J}^j_{TD}\delta_{ji} + \sum_{j=1}^{N} \bar{J}^d_{j,\,j+1}\delta_{ji}\delta_{j+1,i} && \textit{region near the tip } i \\ & && 0 \le \kappa r \le 1 \\ \bar{J} &= \bar{J}^{GO} + \sum_{j=1}^{N} \bar{J}^j_{TD} + \sum_{j+1}^{N} \bar{J}^d_{j,\,j+1} && \textit{elsewhere} \end{aligned}\right\} \quad (13)$$

where

$$\delta_{ij} = \begin{cases} 0 \textit{ for } j = i \\ 1 \textit{ for } j \neq i \end{cases} \quad (14)$$

$\bar{J}^{j}_{TD}$ is the diffracted current from the tip j

$\bar{J}^{d}_{j,j+1}$ is the diffracted current from the edge j, j+1.

Note that with the above expressions we do not neglect the interaction between the vertices.

By using the EFIE as in the previous section, except that the number of sample or match points will be N times (N is the number of vertices) the number of the unknowns used in the angular section case, we can determine the coefficients A_i and B_i.

Due to the nature of our solution it is easy to show, as in Reference 7, that the current near the vertices has "edge condition" properties. This means that the current normal to the edge vanishes as the square root of the normal distance and the current parallel to the edge has a square root singularity. In Reference 7 there is a Figure D.2 (5a in this paper) which shows the rectangular component of the current near the tip of a quarter plane. However, if we calculate and plot the current in polar form rather than in rectangular form, we will easily see the spike at the corner (Figure 5b).

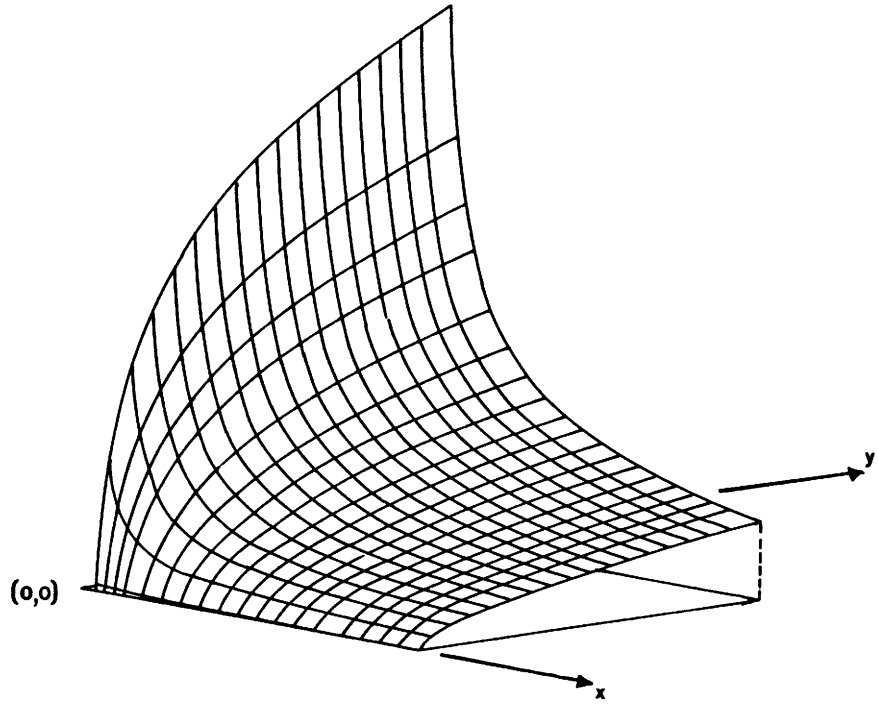

Figure 5a The rectangular J_y component of the current near the tip of a quarter plane.

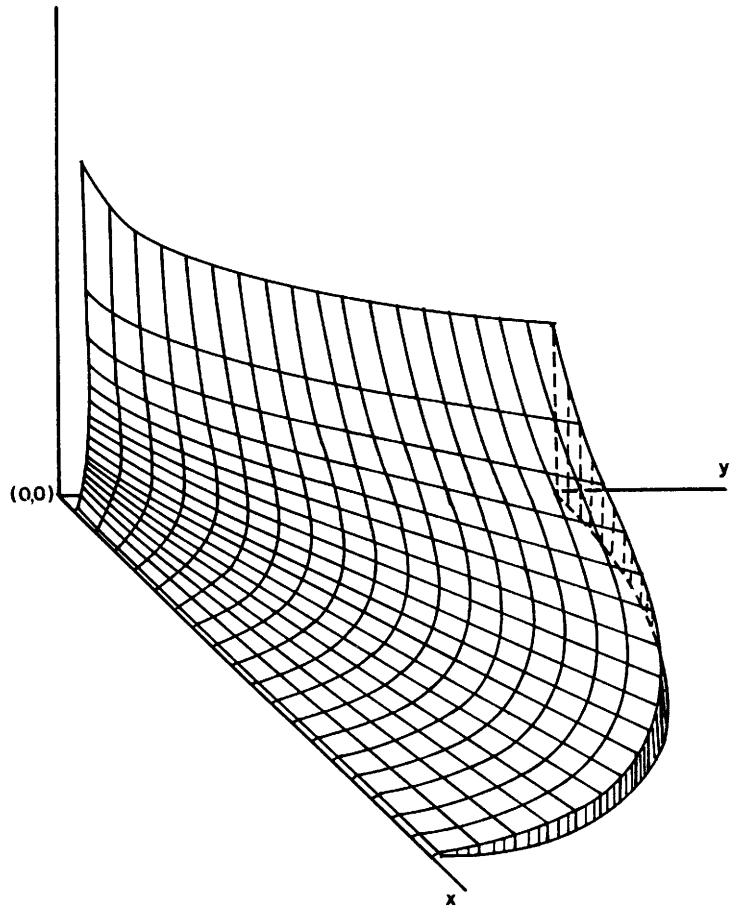

Figure 5b The rectangular J_y component of the current near the tip of a quarter plane (plotted along the radial lines).

Looking at the current on a 0.5λ by 0.5λ plate, we see the current in Figure 5c calculated in rectangular form and in Figure 5d calculated in polar form at the vertices. (Note that the vertical scales in Figures 5c and 5d are not the same.) A further difference between Figures 5c and 5d is that the solution in Reference 7 does not allow the current to be calculated right up to the vertices as a careful examination of Figure 5c shows. From Figures 5c and 5d it is easy to draw two different conclusions about the current distribution. However, we maintain that both distributions are "correct", it is only that the one in Figure 5c is incomplete and thus omits the spike on the four corners. the existence of the current spikes is also required by the mathematics in Equations (5) and (7). Figure 5a shows that as we approach to the edge y, the current has close to it a curved distribution. Figure 5b shows that close to the edge the current tends to a concave distribution.

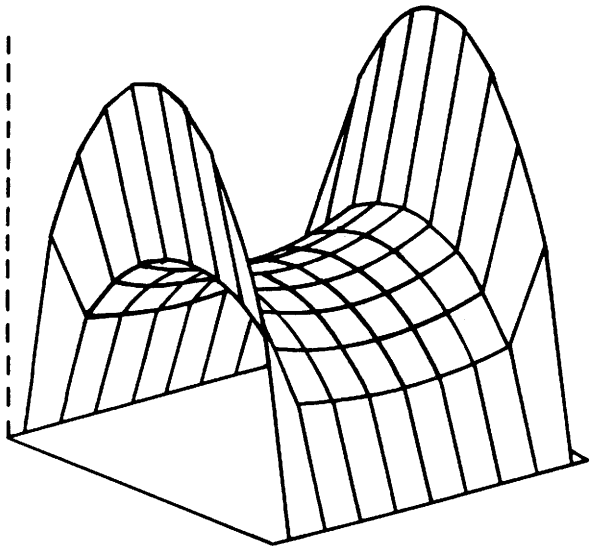

Figure 5c The rectangular coordinate current on a 0.5λ square plate.

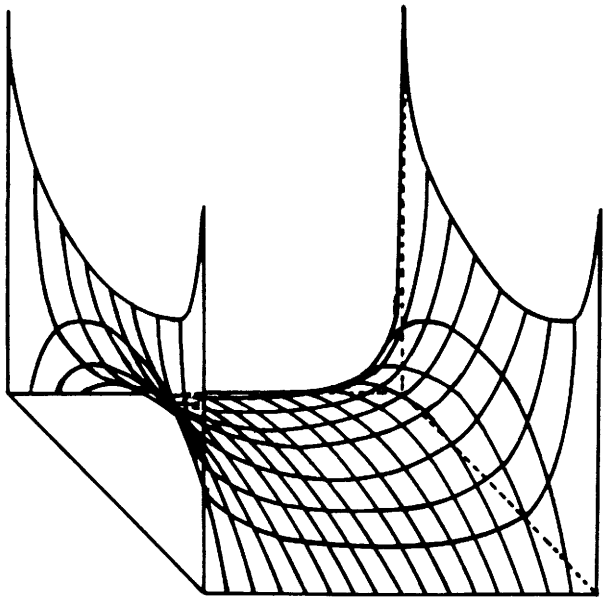

Figure 5d The polar coordinate current on a 0.5λ square plate.

Results for a 1λ *by* 1λ square plate are shown in Figure 6 for plane wave incidence. The current in Figures 6a and 6b may be compared with that presented in References 6 and 7 for this size plate. Figure 6 agrees with that in Reference 6 but not with that in Reference 7 as we have discussed above. For larger plates our work disagrees with Reference 6 (the method in Reference 7 is not useful for large plates). In Reference 6, Ko and Mittra observed no singularity at the corners for 2λ by 2λ and 3λ by 3λ plates. We believe, that because the interaction between corners is small for large plates, it is inevitable that a strong singularity be observed in current there. This conclusion is the opposite of that in Reference 6. It may be that the solution in Reference 6 is not converged for large plates.

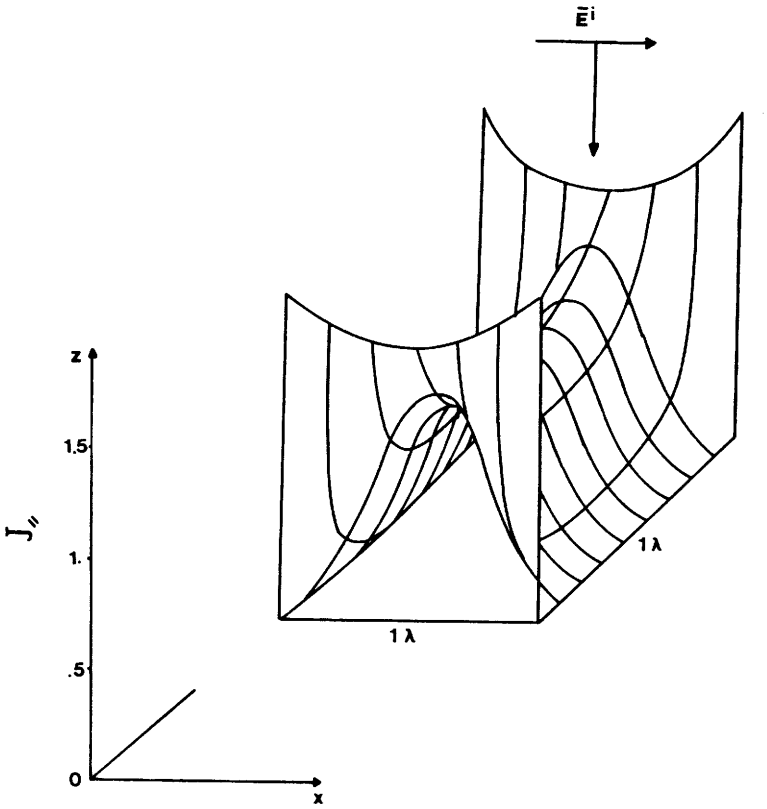

Figure 6a Current distribution on a 1λ square plate.

At this time we might comment that previously in Reference 8 we did not include the interaction between the vertices and did not obtain the correct cross polarized currents. The cross polarized currents in Reference 8 vanished only along one symmetry axis whereas in

Figure 6b we see that the current vanishes along both symmetry axes as it must from physical considerations. From this we conclude that the interaction between vertices is important.

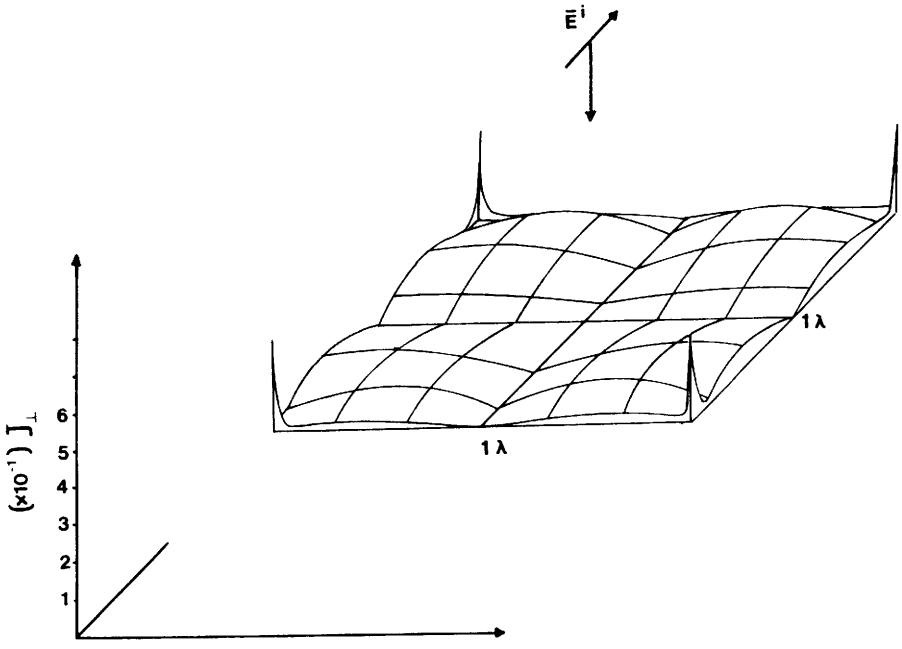

Figure 6b Cross-polarized current on a 1λ square plate.

Figure 7 shows the current on a 2.5λ by 2.5λ square plate where the same properties are shows as before. In Figure 7b the edge condition of the current is not shown for purposes of clarity. Finally, Figure 8 shows the far field pattern of a short monopole or stub radiator at the center of 8λ square ground plane. The result is compared with an unpublished result by Marhefka who obtained his result using the UTD with vertex diffraction [9]. The two results are seen to be in very close agreement. Also in the same figure is shown the far field without using tip diffraction. From this we can see the importance of tip diffraction.

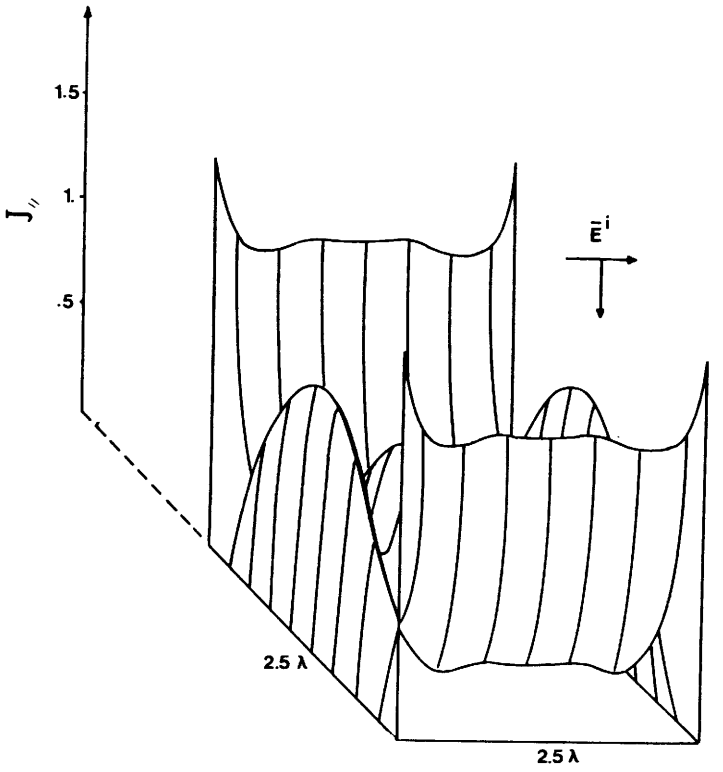

Figure 7a Current distribution on a 2.5λ square plate.

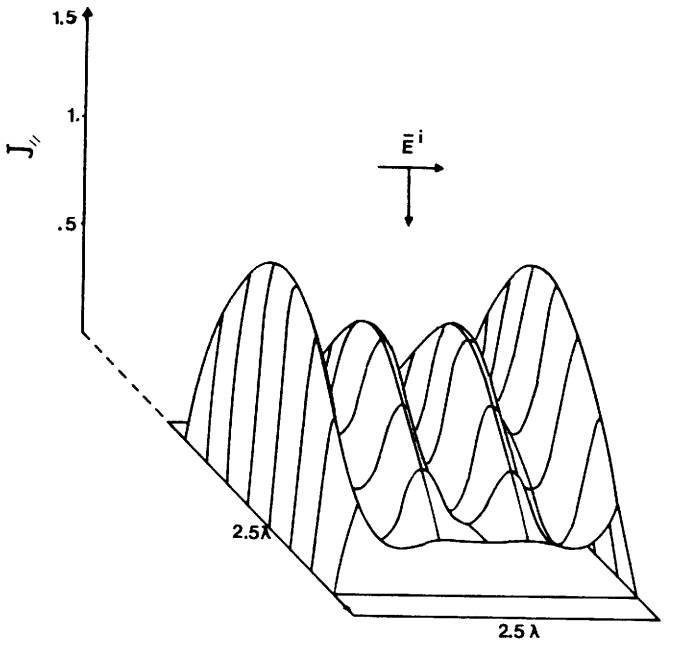

Figure 7b Current distribution on a 2.5λ square plate without the edge condition.

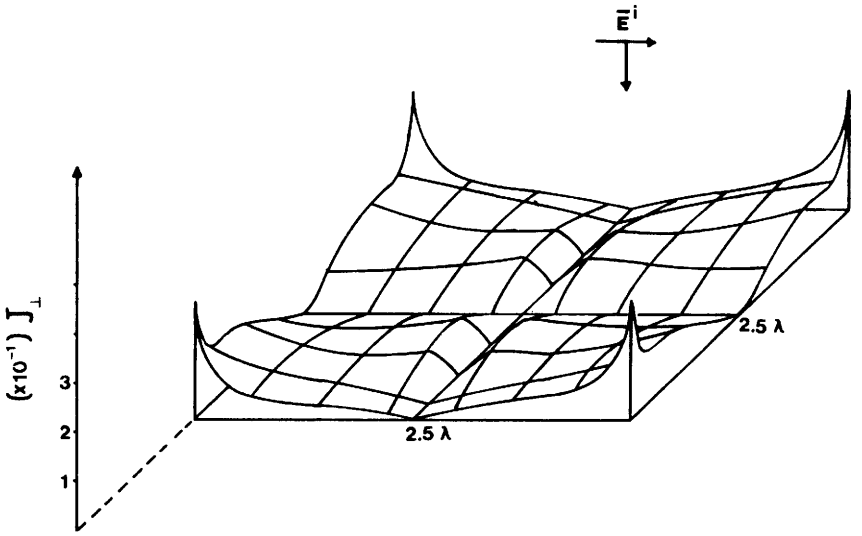

Figure 7c Cross-polarized current on a 2.5λ square plate.

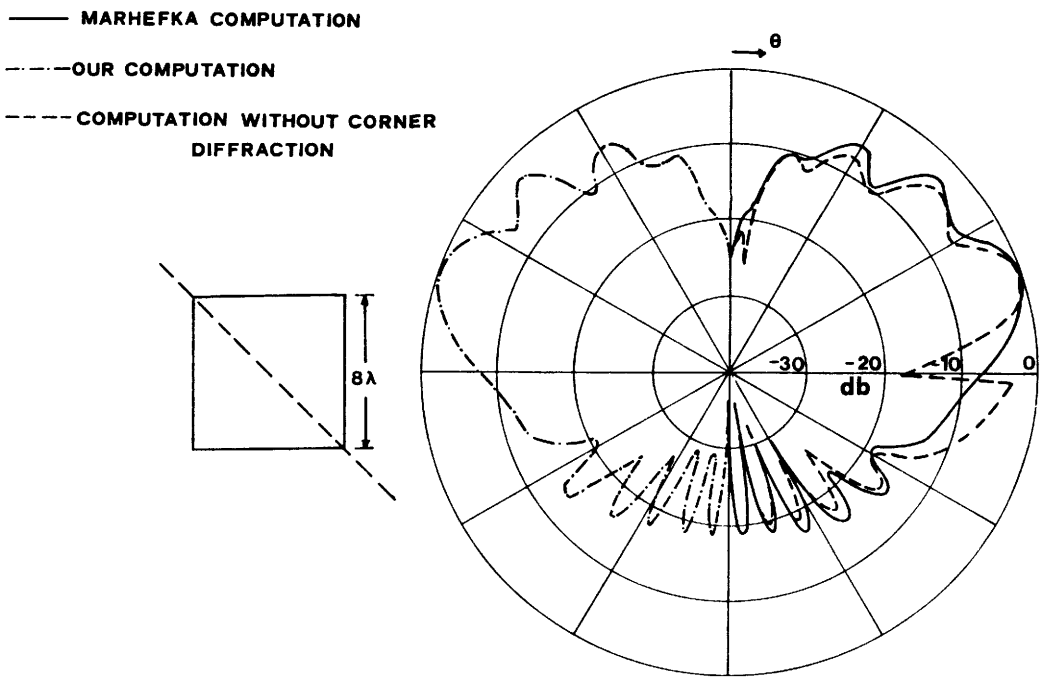

Figure 8 Far field pattern in the plane diagonally through an 8λ square plate with a shore monopole in the center.

IV. SUMMARY

In this paper we have shown that only the first few eigenvalues of the plane angular sector problem contribute to the current in a region very close to the tip itself. Beyond this region the UTD may be used to obtain the current thereby overcoming the need to use large numbers of eigenvalues and eigenfunctions.

We then applied the combined eigenfunction-UTD technique to find the currents and resulting radiation fields. To demonstrate the validity of the solution, the radiation pattern of a monopole at the center of a square plate is compared with that calculated with an unpublished UTD solution which includes vertex diffraction. Two independent results are in very close agreement.

REFERENCES

1. R. Satterwhite and R.G. Kouyoumjian, "Electromagnetic Diffraction by a Perfectly-Conducting Plane Angular Sector," ElectroScience Laboratory, Ohio State University, Columbus, Ohio, Technical Report 2183-2, 1970.

2. R. Satterwhite, "Diffraction by a Quarter Plane, the Exact Solution, and Some Numerical Results," IEEE Transaction on Antennas and Propagation, AP-22, No.3, May 1974, pp. 500-503.

3. J.N. Sahalos and G.A. Thiele, "Periodic Lame Functions and Applications to the Diffraction by a Plane Angular Sector," Canadian Journal of Physics, Vol. 61, No. 12, 1983, pp. 1583-1591.

4. L. Kraus, "Diffraction by a Plane Angular Sector," Thesis, New York University, 1955.

5. L. Kraus and L. Levine, "Diffraction by an Elliptic Cone," Communications on Pure and Applied Mathematics, Vol. XIV, 1961, pp. 49-68.

6. W.L. Ko and R. Mittra, "A New Approach on a Combination of Integral Equation and Asymptotic Techniques for Solving Electromagnetic Scattering Problems," IEEE Transactions on Antennas and Propagation, Vol. AP-25, Mar. 1977, pp. 187-197.

7. D.R. Wilton, et al., "Numerical Solutions for Scattering by Rectangular Bent Plate Structures," Dept. of Electrical Engineering, University of Mississippi, Technical Report, Oct. 1976.

8. J.N. Sahalos and G.A. Thiele, "A Hybrid UTD-Eigenfunction Method for Scattering by a Vertex," ElectroScience Laboratory, Ohio State University, Columbus, Ohio, Technical Report 711353-3, June 1980.

9. F.A. Sikta, W.D. Burnside, T. Chu and L. Peters, Jr., "First-Order Equivalent Current and Corner Diffraction Scattering from Flat Plate Structures, IEEE Transactions on Antennas and Propagation, Vol. AP-31, July 1983, pp. 584-589.